Available online at www.sciencedirect.com
SCIENCE DIRECT®
Journal of Electron Spectroscopy and Related Phenomena 149 (2005) 29–36
JOURNAL OF ELECTRON SPECTROSCOPY and Related Phenomena
www.elsevier.com/locate/elspec

Experimental and theoretical investigations into the electronic structure of cyclohexene by electron momentum spectroscopy

X.G. Ren, C.G. Ning, S.F. Zhang, G.L. Su, B. Li, H. Zhou, Y.R. Huang, G.Q. Li, J.K. Deng *

Department of Physics and Key Laboratory of Atomic and Molecular, NanoSciences of MOE, Tsinghua University, Beijing 100084, PR China

Received 14 March 2005; received in revised form 8 June 2005
Available online 15 August 2005

Abstract

The orbital electron momentum distributions and binding energy spectrum of the valence shell of cyclohexene (C_6H_{10}) were investigated by a binary (e, 2e) electron momentum spectrometer at an impact energy of 1200 eV plus the binding energy. The experimental momentum distributions are compared with the theoretical momentum distributions obtained by using Hartree–Fock and density functional theory methods. The agreements between theory and experiment for the shape and intensity are generally good. Some discrepancies between experimental data and theoretical calculations of the momentum distributions could be due to the possible distorted-wave effects and the conformation variety of cyclohexene. The pole strengths of the main ionization peaks from the orbitals in the inner valence region are estimated.

Keywords: Electron momentum spectroscopy; Cyclohexene; Complete valence orbitals; Hartree–Fock; Density functional theory

1. Introduction

Electron momentum spectroscopy (EMS), or binary (e, 2e) spectroscopy, is now a powerful tool to investigate electronic structures of atoms and molecules due to its unique ability to measure the momentum distributions for orbitals. EMS is based on kinematically complete ionization experiments initiated by high energy electrons. The momentum distributions could provide stringent test of theoretical wavefunctions at the Hartree–Fock (HF) level and also correlated treatments such as configuration interaction (CI) methods and density functional theory (DFT). In addition, EMS is also a sensitive probe of molecular structure, chemical bonding and reactivity in the low momentum region [1–3].

Cyclic unsaturated hydrocarbon cyclohexene (C_6H_{10}), also known as 1,2,3,4-tetrahydrobenze, is a chemical raw material and organic solvent [4,5] and organic–semiconductor surface chemistry reactant [6,7]. Cyclohexene is also one of the fundamental structures in the stereochemistry of organic compounds. Its molecular geometry and conformational characteristics of this molecule were extensively investigated using various experimental [8,9] and theoretical [8–11] methods. The vertical potentials of C_6H_{10} except the innermost valence orbital have also been investigated by photoelectron spectroscopy [12,13].

In the present work the binding energy spectrum (4–34 eV) and momentum distributions for the complete valence shell of cyclohexene have been measured at the impact energy of 1200 eV plus binding energy. Theoretical momentum distributions for were calculated by using the target Hartree–Fock approximation (THFA) and also the target Kohn–Sham approximation (TKSA) of DFT [1–3].

2. Experimental and theoretical background of EMS

An energy-dispersive electron momentum spectrometer with a symmetric non-coplanar geometry was used in this work. The details of the spectrometer constructed at Tsinghua

* Corresponding author. Tel.: +86 16278 5594; fax: +86 16278 1604.
E-mail address: djk-dmp@mail.tsinghua.edu.cn (J.K. Deng).

0368-2048/$ – see front matter © 2005 Elsevier B.V. All rights reserved.
doi:10.1016/j.elspec.2005.06.005

University have been reported previously [14]. Briefly, in this experiment the relative (e, 2e) cross section for electron impact ionization (i.e., the binary (e, 2e) reaction) is measured by detecting the two outgoing electrons (scattered and ionized) in coincidence. A newly developed multi-parameter data acquisition system based on universal serial bus (USB) interface [15] was used for data acquisition and experimental controls in this EMS spectrometer. The particular kinematics of the experiment is chosen in such a way as to provide a straightforward relation between some variable kinematic parameters and the momentum of the ionized electron prior to knock-out. For this purpose the symmetric non-coplanar kinematics [1–3] is the most convenient and frequently used experimental configuration.

In the symmetric non-coplanar scattering geometry, the two outgoing electrons are selected to have equal polar angles ($\theta_1 = \theta_2 = 45^\circ$) relative to the direction of incident electron beam. The relative azimuthal angle ϕ between the two outgoing electrons is varied by rotating one of the analyzers over the range of 0° to $\pm 30^\circ$ around the incident beam axis. Under these high impact energy and high momentum transfer conditions, the plane wave impulse approximation (PWIA) provides a good description of the collision and the ionized electron essentially undergoes a clean 'knock-out' collision. Within the PWIA, the momentum p of the ejected electron prior to knockout is related to the azimuthal angle by

$$p = [(2p_1 \cos\theta_1 - p_0)^2 + (2p_1 \sin\theta_1 \sin(\phi/2))^2]^{1/2} \quad (1)$$

where p_1 and p_0 are the momenta of the outgoing and incident electrons, respectively. The EMS reaction theory is based on several approximations [1–3], through which the binary (e, 2e) cross-section is related to the electronic structure of the target. Of these approximations the binary encounter approximation assumes that the interaction operator depends only on the coordinates of the two electrons immediately involved in ionization, with all other particles being treated as "spectators" and the incoming and both outgoing electrons are represented by plane waves. In order to ensure the validity of these approximations the experiment has to be conducted under high electron impact energy and the use of particular kinematics. When these experimental conditions are met it has been shown that the kinematic factors are effectively constant [16] and that the relative (e, 2e) cross-section σ_{EMS} is then proportional to the spherically averaged momentum distribution of the corresponding Dyson orbital:

$$\sigma_{\mathrm{EMS}} \propto \int \mathrm{d}\Omega |\langle p\Psi_{\mathrm{f}}^{N-1} | \Psi_{\mathrm{i}}^{N} \rangle|^2 \quad (2)$$

where p is the momentum of the target electron prior to ionization. $|\Psi_{\mathrm{f}}^{N-1}\rangle$ and $|\Psi_{\mathrm{i}}^{N}\rangle$ are the total electronic wavefunctions for the final ion state and the target molecule ground (initial) state, respectively. The $\int \mathrm{d}\Omega$ represents the spherical average due to the randomly oriented gas phase target.

Eq. (2) can be greatly simplified by using the target Hartree–Fock approximation (THFA), in which the Dyson orbital can be approximated with an initial state canonical HF orbital. Then the σ_{EMS} becomes

$$\sigma_{\mathrm{EMS}} \propto \int \mathrm{d}\Omega |\Psi_j^{\mathrm{HF}}(p)|^2 \quad (3)$$

where $|\Psi_j^{\mathrm{HF}}(p)\rangle$is the one-electron momentum space canonical HF orbital wave function for the jth electron.

The Kohn–Sham DFT provides the alternative approach to approximating the Dyson orbital in Eq. (2). The target Kohn–Sham approximation (TKSA) has been shown to give a good description of the experimental momentum profiles of lots of molecules measured by EMS [3]. The TKSA gives a result similar to Eq. (3) with the canonical HF orbital replaced by a momentum space Kohn–Sham orbital (KSO) $|\Psi_j^{\mathrm{KS}}(p)\rangle$:

$$\sigma_{\mathrm{EMS}} \propto \int \mathrm{d}\Omega |\Psi_j^{\mathrm{KS}}(p)|^2 \quad (4)$$

A more detailed description of the TKSA method can be found elsewhere [17]. The integrals in Eqs. (3) and (4) are known as the spherically averaged one-electron momentum distribution (MD).

3. Calculations

Spherically averaged theoretical momentum profiles of cyclohexene were calculated within PWIA and THFA or TKSA with the HEMS program developed at UBC. The HEMS program first calculates a Fourier transform of a given position space molecular orbital and then performs spherical averaging of its square. The position space molecular orbitals were calculated using the GAUSSIAN'98 program. The canonical HF orbitals for cyclohexene were calculated using the 6-31G, 6-311++G** and AUG-CC-PVTZ basis sets. The KSOs were achieved by running DFT calculations utilizing the B3LYP hybrid gradient polarization functionals with these basis sets. In order to compare the calculated cross-sections with the experimental momentum profiles the effects of the finite spectrometer acceptance angles in both θ and ϕ ($\Delta\theta = \pm 0.6^\circ$ and $\Delta\phi = \pm 1.2^\circ$) and energy resolution of 1.2 eV (FWHM) obtained by the measurement of argon 3p state were included by using the Gaussian-weighted planar grid (GWPG) method [18].

An outer valence shell Green function (OVGF) [19] calculation of ionization potentials for outer valence orbitals of cyclohexene has been carried out using 6-311+G* basis set, as shown in Table 1. OVGF calculation also gives the pole strengths [3] for outer valence orbitals, which are listed in Table 1.

4. Results and discussion

Cyclohexene has mainly C_2 point group symmetry according to molecular orbital theory [10]. Its ground state elec-

Table 1
Ionization energies (eV) and pole strength for cyclohexene

Orbital	Experimental results			Theoretical calculations[a]	
	PES[b]	PES[c]	EMS[d]	Ionization potential	Pole strength
8b	8.94		9.05	8.934	0.912
7b	10.7			10.623	0.910
9a	11.3		11.35	11.026	0.911
8a	11.7			11.596	0.918
6b	12.8			12.896	0.905
5b	13.2			13.177	0.908
7a	13.5		13.33	13.101	0.894
6a	13.8			13.824	0.902
4b	14.5			14.579	0.904
5a	15.2			15.328	0.900
4a	16.3			16.469	0.881
3b		16.73	15.89	17.200	0.881
2b		19.29	19.33		
3a		19.83			
1b		22.78	22.61		
2a		23.49			
1a			25.30		

[a] OVGF with 6-311+G* in this work.
[b] From Ref. [12].
[c] From Ref. [13].
[d] This work.

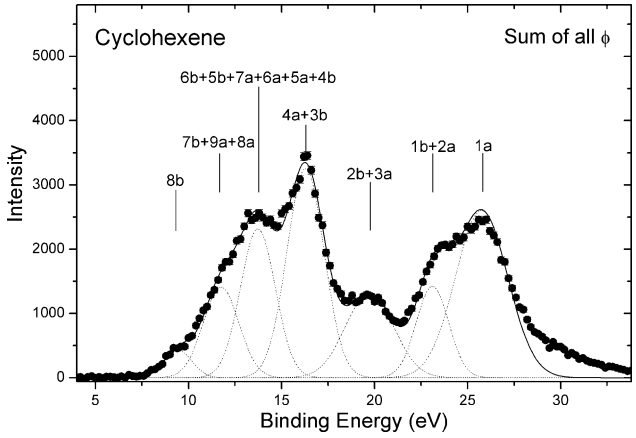

Fig. 1. Binding energy spectrum of cyclohexene from 4 to 34 eV for the summed all ϕ angles. The dashed and solid lines represent individual and summed Gaussian fits, respectively.

tronic configuration can be written as

$$(\text{core})^{12}\underbrace{(1a)^2(2a)^2(1b)^2(3a)^2(2b)^2}_{\text{inner valence}},\qquad \underbrace{(3b)^2(4a)^2(4b)^2(5a)^2(6a)^2(7a)^2(5b)^2(6b)^2(8a)^2(9a)^2(7b)^2(8b)^2}_{\text{outer valence}}$$

All the molecular orbitals are either a- or b-type. The assignment of the order of occupation for these valence orbitals has been discussed in Refs. [12,13].

4.1. Binding energy spectrum

To obtain the experimental momentum profiles, 12 binding energy spectra over the energy range of 4–34 eV were collected at the out-of-plane azimuthal angles $\phi = 0^\circ$, 1°, 2°, 3°, 4°, 6°, 8°, 10°, 12°, 14°, 16° and 21° in a series of sequential repetitive scans. The valence shell binding energy spectrum of cyclohexene for the summed over all ϕ angles is shown in Fig. 1. This spectrum is fitted with a set of individual Gaussian peaks whose widths are combination of the instrumental energy resolution and the corresponding Franck–Condon widths estimated from high resolution PES data [12,13]. The relative energy spacings of the Gaussian peaks were estimated from the vertical ionization potentials in high resolution PES [12], small adjustments have been applied to compensate the asymmetries of the shapes of the Frank–Condon profiles. The fitted Gaussians for individual peaks are indicated by dashed lines while their sum, i.e., the overall fitted spectrum, is represented by the solid line.

The PES spectra of the outer valence orbital region using He(I) radiation source have been reported in Ref. [12]. In the PES work, the vertical ionization potential of the 8b HOMO was 8.94 eV, and the 7b, 9a, 8a, 6b, 5b, 7a, 6a, 5a, 4b and 4a orbitals were determined to be 10.7, 11.3, 11.7, 12.8, (13.5), 13.2, 13.8, (14.5), 15.2 and 16.3 eV, respectively. These PES studies were extended by Streets and Potts [13] which include some of the inner valence region of C_6H_{10} and the ionization potentials at 16.73, 19.29, 19.83, 22.78 and 23.49 eV were assigned to the 3b, 2b, 3a, 1b and 2a orbitals, respectively.

In the present EMS work, seven structures could be identified in the binding energy spectrum of Fig. 1. The vertical ionization potential of 8b orbital is determined to be 9.05 eV. The averaged vertical ionization potentials of the (7b + 9a + 8a), (6b + 5b + 7a + 6a + 5a + 4b) and (4a + 3b) are determined to be 11.35, 13.33 and 15.89 eV, respectively. The averaged ionization potentials of (2b + 3a) and (1b + 2a) inner valence orbitals were determined to be 19.33 and 22.61 eV, respectively. One more inner valence orbital, 1a, was observed in the measured ionization spectrum and its ionization energy was determined to be 25.30 eV in the present work. Some rather weak satellite structure above 27.5 eV in the binding energy spectrum are observed which could be due to many-body correlation effects in the target or in the final state of residual ion.

4.2. Momentum profiles

Experimental momentum profiles (XMPs) were extracted by deconvolving the same peak of the sequentially obtained angular correlated binding energy spectra, and therefore the relative normalization for the different transitions is maintained. The Gaussian fitting procedure for the binding energy spectra is used to determine the relative intensities of the various transitions at each azimuthal angle ϕ. The experimental momentum profile corresponding to a particular final ion state is obtained by plotting the area under the corresponding fit-

ted peak for each electronic state of the ion as a function of momentum p (also ϕ angle). The measured momentum profiles are not absolute, so the obtained relative magnitude needs to be normalized by an absolute scale [1]. Usually, the normalization factor is determined by normalizing the experimental and theoretical momentum distributions of the outermost valence ionization to the common intensity scale. In this work we use the HOMO orbital to determine this normalization factor. The theoretical momentum distribution used for normalization is calculated by DFT-B3LYP method employing AUG-CC-PVTZ basis set. This normalization is chosen because the HOMO orbital has large spectroscopic pole strength (i.e., little splitting, see Table 1) and the HOMO experimental momentum distribution is in good agreement for shape with the calculated curve. The same normalization factor is also preserved for the other experimental momentum profiles of cyclohexene valence orbitals in Figs. 3–9.

Fig. 2 shows the experimental momentum profile for the 8b orbital of cyclohexene. The theoretical momentum profiles have been calculated using the HF and DFT-B3LYP methods with 6-31G, 6-311++G** and AUG-CC-PVTZ basis sets. The 8b orbital has a "p-type" momentum distribution, which is the case shown in our experiment. It can be seen from this figure that the calculation inclusion of dynamic electron correlation effects (curve 4) could provide proper descriptions of the chemically important larger r (lower p) region of cyclohexene HOMO. The detailed description can be found in Ref. [20]. The momentum distribution denotations of "p-type" and the next usage of "s-type" are similar with the atomic argon 3p and 3s states, respectively [3].

Experimental and theoretical momentum profiles for the summed 7b, 9a and 8a orbitals are shown in Fig. 3. Both the experimental and theoretical momentum profiles display a mainly "s-type" distribution with a secondary maximum at ∼1.15 a.u. The HF and DFT-B3LYP calculations are consistent in shape with the summed experimental momentum profile (XMP). The theoretical momentum profiles indicate that the 8a orbital (curve 7) has a mainly "s-type" with a secondary "p-type" distribution while the 9a and 7b orbitals (curves 8 and 9) have the "p-type" distribution with a secondary maximum as shown in Fig. 3. However, there is a discrepancy between experimental data and summed theoretical momentum profiles in low momentum region. Such discrepancy in the low momentum region is probably due to 'contamination' from the neighbouring relatively intense transition caused by the uncertainty in the curve fitting procedures.

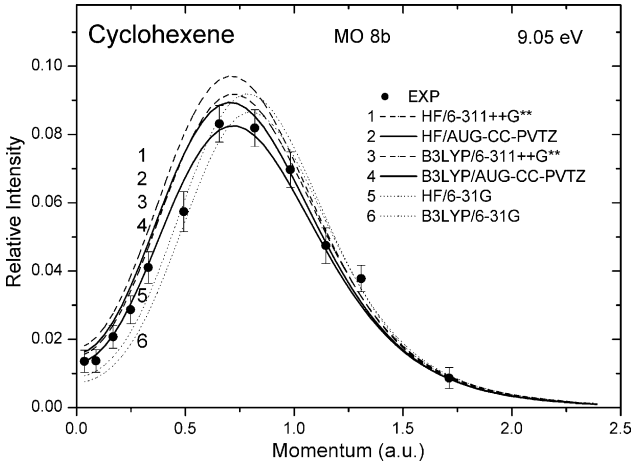

Fig. 2. Experimental and calculated electron momentum distributions for the 8b orbital of cyclic unsaturated cyclohexene. The theoretical momentum profiles are calculated by using HF (curves 1, 2 and 5) and DFT-B3LYP (curves 3, 4 and 6) methods with the 6-311++G**, AUG-CC-PVTZ and 6-31G basis sets, respectively.

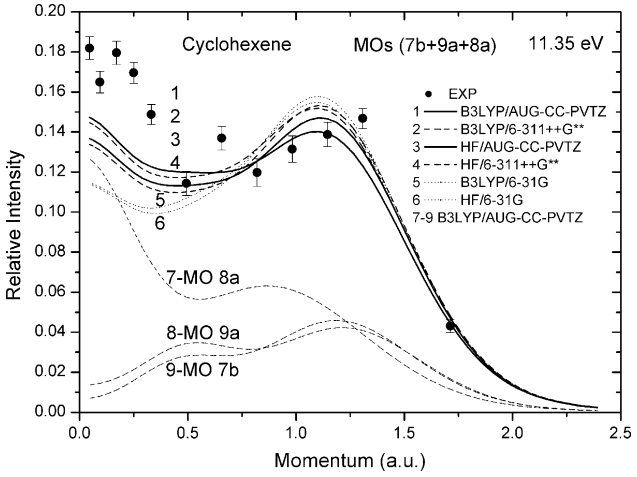

Fig. 3. Experimental and calculated electron momentum distributions for the summed and individual orbitals of the 7b, 9a and 8a of cyclohexene. The summed TMPs are calculated by using HF (curves 3, 4 and 6) and DFT-B3LYP (curves 1, 2 and 5) methods with the AUG-CC-PVTZ, 6-311++G** and 6-31G basis sets, respectively. The TMPs of individual orbitals are calculated by using the DFT-B3LYP method with the AUG-CC-PVTZ basis set (curves 7–9).

This explanation seems to be supported from the comparison for the XMP of the summed 6b, 5b, 7a, 6a, 5a and 4b orbitals with the calculations in Fig. 4, which is the third band located at 13.33 eV in the binding energy spectrum (Fig. 1). Some discrepancy between experiment and theory in the low momentum region can be observed in Fig. 4. And the theoretical calculations can reasonably reproduce the experimental data above 0.5 a.u. In order to further investigate the explanation, the summed experimental data of the 8b, (7b + 9a + 8a) and (6b + 5b + 7a + 6a + 5a + 4b) orbitals was compared with the summed theoretical calculations in Fig. 5. Again, the summed theoretical calculations give a reasonable description for the summed XMP above 0.5 a.u., and underestimate the experimental data in low momentum region. This indicates that the discrepancy between experimental data and theoretical calculations below 0.5 a.u. for the summed (7b + 9a + 8a) orbitals (see Fig. 3) is not mainly due to a possible error in the curve fitting and deconvolution procedures. Some other sources could be due to the possible distorted wave effects in molecules and the possibly presence of other conformers of cyclohexene in the EMS measurements [21].

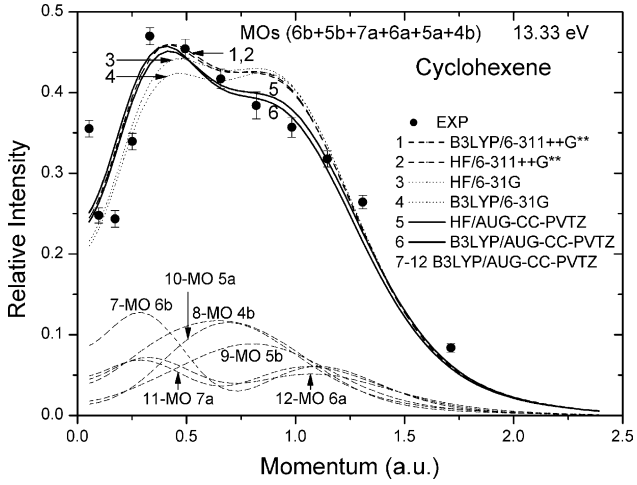

Fig. 4. Experimental and calculated electron momentum distributions for the summed and individual orbitals of the 6b, 5b, 7a, 6a, 5a and 4b of cyclohexene. The summed TMPs are calculated by using HF (curves 2, 3 and 5) and DFT-B3LYP (curves 1, 4 and 6) methods with the 6-311++G**, 6-31G and AUG-CC-PVTZ basis sets, respectively. The TMPs of individual orbitals are calculated by using the DFT-B3LYP method with the AUG-CC-PVTZ basis set (curves 7–12).

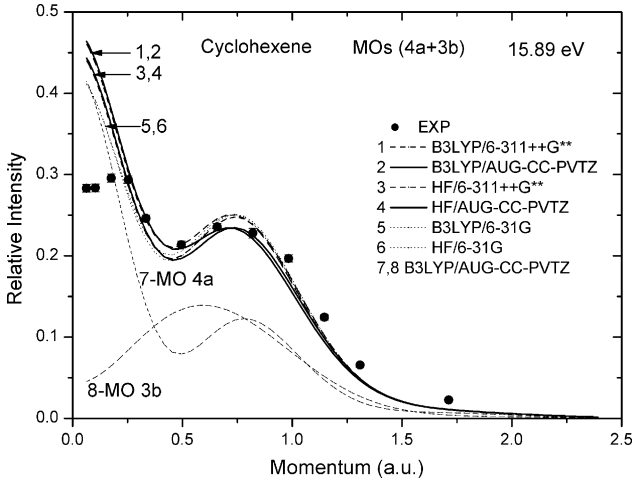

Fig. 6. Experimental and calculated electron momentum distributions for the summed and individual orbitals of the 4a and 3b of cyclohexene. The summed TMPs are calculated by using HF (curves 3, 4 and 6) and DFT-B3LYP (curves 1, 2 and 5) methods with the 6-311++G**, AUG-CC-PVTZ and 6-31G basis sets, respectively. The TMPs of individual orbitals are calculated by using the DFT-B3LYP method with the AUG-CC-PVTZ basis set (curves 7 and 8).

For the third band in Fig. 1 the ionization peaks are not completely resolved due to the low energy resolution of the current EMS spectrometers. The calculated momentum distributions of the 6b, 5b, 7a, 6a, 5a and 4b orbitals are summed, as indicated by curves 1–6 in Fig. 4. The 5b, 5a and 4b orbitals have the "p-type" distributions while 6b, 7a and 6a orbitals have the "p-type" distribution with a secondary maximum, as shown by curves 7–12 in Fig. 4. The comparison of the summed XMPs with various calculations in Fig. 4 shows that the theoretical momentum profiles obtained using HF and DFT-B3LYP methods with the AUG-CC-PVTZ basis set (curves 5 and 6) can reproduce the experimental data reasonably well, particularly in the momentum range above 0.5 a.u., and the other calculations with 6-311++G** and 6-31G basis sets (curves 1–4) have a relatively higher intensity than the experimental data in the above 0.5 a.u. momentum.

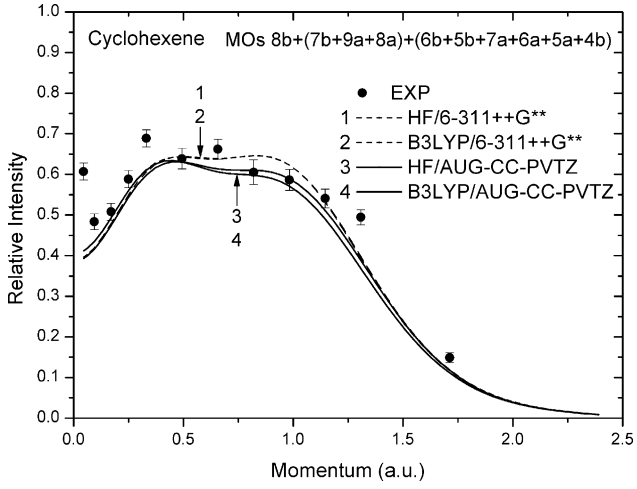

Fig. 5. Experimental and calculated electron momentum distributions for the summed 8b, (7b + 9a + 8a) and (6b + 5b + 7a + 6a + 5a + 4b) orbitals of cyclohexene. The solid circles represent the experimental measurements. The TMPs are calculated by using HF (curves 1 and 3) and DFT-B3LYP (curves 2 and 4) methods, respectively.

The experimental and theoretical momentum distributions of the 4a and 3b orbitals positioned at 15.89 eV are shown in Fig. 6. The 3b orbital has a "p-type" character while the 4a orbital shows an "s-type" distribution with a secondary maximum, as indicated by curves 7 and 8 in Fig. 6. The summed momentum profile is a mixed "s-type" with a secondary "p-type" distribution. It can be seen from the comparison in Fig. 6 that the summed theoretical profiles calculated by HF and DFT with AUG-CC-PVTZ basis set reproduce the XMP well except the low momentum range (below 0.2 a.u.). The comparison between the experimental data and theoretical calculations in Fig. 6 shows that all six calculations significantly overestimate the experimental intensity in the region below 0.2 a.u. momentum. This discrepancy between theory and experimental data may be due to the uncertainty in the deconvolution procedure. However, it can be seen from the low momentum region (also the low ϕ) such as $\phi = 1^\circ$ binding energy spectrum in the Letter [20] published previously that the (e, 2e) cross section of the summed (4a + 3b) orbitals is larger than the neighbouring bands at 13.33 and 19.33 eV. Therefore, the significant discrepancy between experiment and theory in the low momentum region could not mainly due to the influence from the neighbouring band in the deconvolution procedures. Another possible source for this discrepancy could be due to the presence of other conformations on the larger cyclic unsaturated hydrocarbon of cyclohexene in the vacuum chamber of the (e, 2e) spectrometer. The detailed discussions of molecular conformations with EMS have been made in Ref. [21].

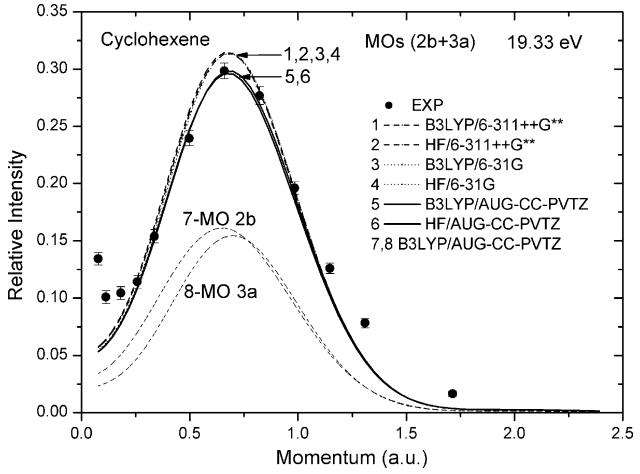

Fig. 7. Experimental and calculated electron momentum distributions for the summed and individual orbitals of the 2b and 3a of cyclohexene. The summed TMPs are calculated by using HF (curves 2, 4 and 6) and DFT-B3LYP (curves 1, 3 and 5) methods with the 6-311++G**, 6-31G and AUG-CC-PVTZ basis sets, respectively. The TMPs of individual orbitals are calculated by using the DFT-B3LYP method with the AUG-CC-PVTZ basis set (curves 7 and 8).

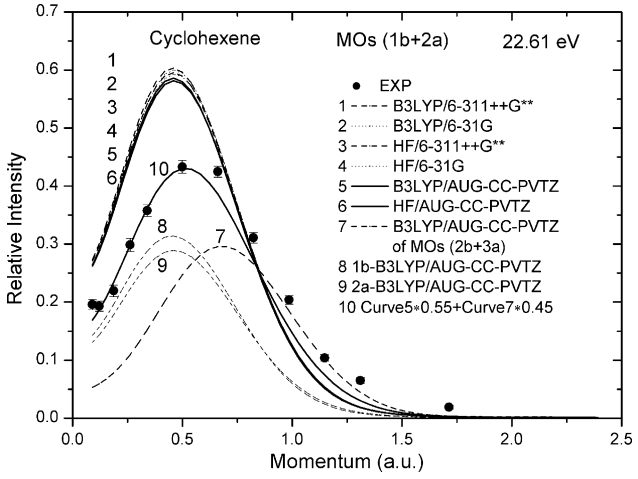

Fig. 8. Experimental and calculated electron momentum distributions for the summed and individual orbitals of the 1b and 2a of cyclohexene. The summed TMPs are calculated by using HF (curves 3, 4 and 6) and DFT-B3LYP (curves 1, 2 and 5) methods with the 6-311++G**, 6-31G and AUG-CC-PVTZ basis sets, respectively. The TMPs of individual orbitals are calculated by using the DFT-B3LYP method with the AUG-CC-PVTZ basis set (curves 8 and 9). The curve 10 represents a sum of 0.55× curve 5 plus 0.45× curve 7 of the summed 2b and 3a orbitals (i.e., curve 5 in Fig. 7).

In the inner valence shell the summed momentum distributions of the 2b and 3a orbitals are shown in Fig. 7, peaked at 19.33 eV. The HF and DFT-B3LYP calculations with AUG-CC-PVTZ basis set can reproduce the summed XMPs well in the momentum region above 0.2 a.u. However, there is a discrepancy between theoretical calculations and experimental data below the momentum of 0.2 a.u. and the TMPs underestimate the experimental intensity. Certainly, the discrepancy between experiment and theory in the low momentum region could be possibly due to uncertainties in the curve fitting procedures. Another main source for the experimental data "turn up" in the low momentum range could be the influence of the distorted wave effects since the 2b and 3a orbitals of cyclohexene are the π^*-like molecular orbital. Specifically atomic d-like orbitals and π^*-like molecular orbitals exhibit gerade-type symmetry and as a result zero gradient components of their position space wave functions in the nuclear (atoms) or internuclear (molecules) small r regions [22,23]. Thus, low p components are expected at small r for such orbitals and therefore effects due to distortion of the incoming and outgoing electron waves may be reasonably expected to be manifested in the low p regions of such XMPs [22,23]. The further comparison between the experimental electron momentum profiles for Xe 4d orbitals and the theoretical calculations considering distorted wave effects strongly suggest that these "turn up" effects of (e, 2e) cross sections in the low p region are due to the distorted wave effects [22]. Unfortunately at present distorted wave calculations are possible only for atoms but not for molecules due to the multicenter nature for the molecule targets. Recently, the (e, 2e) experiments in ethylene (C_2H_4) at a wide range of experimental impact energies from 400 to 2400 eV confirmed that the observed "turn up" effects of (e, 2e) cross sections in the low p region of π^*-like molecular orbital are due to the distorted wave effects [23].

The next inner valence band of 1b + 2a orbitals is located at 22.61 eV in the binding energy spectrum shown in Fig. 1. The 1b and 2a orbitals have the "p-type" symmetry and the calculated momentum distributions for the summed 1b and 2a orbital are compared with the experimental data in Fig. 8. It is obvious that all six calculations overestimate the experimental intensity. This indicates that some of the transition intensity from this orbital is located in the higher binding energy range due to the final state electron correlation effects. Another possible source for the discrepancy could probably be due to deconvolution uncertainty. In order to compare the shape of the momentum distribution the DFT-B3LYP calculation with AUG-CC-PVTZ basis set is multiplied by an estimated factors of 0.55 for the summed (1b + 2a) orbitals and 0.45 for the summed (2b + 3a) orbitals, and the summed theoretical momentum distribution is represented by curve 10 in Fig. 8. A good agreement between experiment and theory is then achieved.

The innermost valence orbital located at 25.89 eV, newly observed in the XMP, is mainly due to the ionization of the 1a orbital which has an "s-type" distribution as shown in Fig. 9. The comparison between the experimental data and theoretical calculations shows that all the calculations significantly overestimate the experimental intensity. A strong splitting for the 1a orbital into the higher binding energy region is observed (see Fig. 1) due to the final state electron correlation effects. From above discussion about the (1b + 2a) orbitals it should also be noted that this energy range around 24 eV may include some intensity from the 1b and 2a orbitals. Therefore, estimated factors about of 0.6 and 0.4 are used to

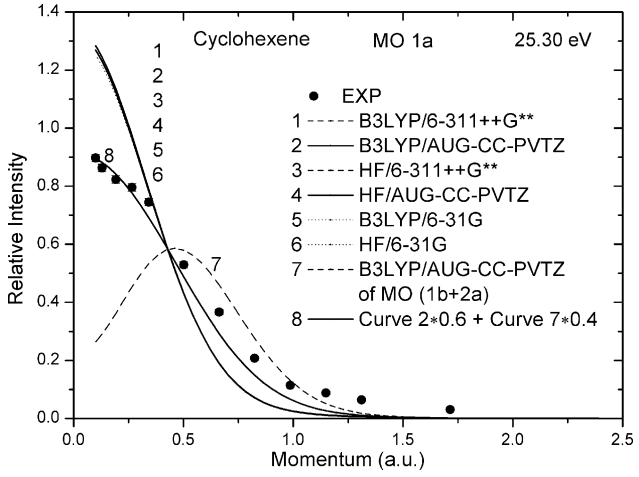

Fig. 9. The experimental and calculated electron momentum distributions for the innermost valence orbital 1a of cyclohexene. The TMPs are calculated by using HF (curves 3, 4 and 6) and DFT-B3LYP (curves 1, 2 and 5) methods with the 6-311++G**, AUG-CC-PVTZ and 6-31G basis sets, respectively. The curve 8 represents a sum of 0.6× curve 2 plus 0.4× curve 7 of the summed 1b and 2a orbitals (i.e., curve 5 in Fig. 8).

multiply the DFT-B3LYP calculation with AUG-CC-PVTZ basis set for the 1a and the summed (1b + 2a) orbitals, respectively. The summed theoretical calculation (curve 8 in Fig. 9) is then compared with the XMP. With the above shape matching scaling factors it can be seen in Fig. 9 that a good fit to experimental data is obtained.

Moreover, by analogy with the algebraic diagrammatic construction (ADC) calculations on the inner valence shell of cyclic hydrocarbons of cyclohexane, cyclopentane [24] and norbornane [25], it should be clear that the innermost 1a, 1b and 2a orbitals of cyclohexene are subject to a severe or complete breakdown of the orbital picture of ionization. Due to the presence of a double bond, this will clearly yield an even stronger dispersion of the ionization intensity over many shake-up lines with individually very limited intensity [25]. Such a breakdown of the orbital picture of ionization could be the reasonable explanations of the very large bandwidth for the 1a, 1b and 2a orbitals in Fig. 1, and the difficulties in the curve fitting and deconvolution procedures for the obtainments of these orbitals momentum distributions.

5. Conclusions

We have reported the first EMS investigations into the complete valence electronic structure and binding energy spectrum of the cyclic unsaturated cyclohexene, in conjunction with the HF and DFT calculations. Momentum distributions for the valence orbital of cyclohexene were measured and compared against a series of PWIA-based calculations using HF and DFT calculations. On the basis of this comparison between the experimental and theoretical momentum distributions, we found that DFT calculations using the B3LYP hybrid functional with the saturated and diffuse basis sets, especially with the AUG-CC-PVTZ basis set, could provide the reasonable representation of the cyclohexene wave function.

Some significant discrepancies between experiment data and theoretical calculations in the (7b + 9a + 8a), (4a + 3b) and (2b + 3a) momentum distributions were observed, which could be mainly due to the possible distorted wave effects in molecules and the presence of different molecular conformations. The inner valence orbitals of cyclohexene are subject to a severe or complete breakdown of the orbital picture of ionization. Due to the presence of a double bond, this will clearly yield an even stronger dispersion of the ionization intensity over many shake-up lines with some estimated spectroscopic strength.

Acknowledgements

Project supported by the National Natural Science Foundation of China under Grant Nos. 19854002, 19774037 and 10274040 and the Research Fund for the Doctoral Program of Higher Education under Grant No. 1999000327.

References

[1] I.E. McCarthy, E. Weigold, Rep. Prog. Phys. 54 (1991) 789.
[2] C.E. Brion, Int. J. Quantum Chem. 29 (1986) 1397.
[3] E. Weigold, I.E. McCarthy, Electron Momentum Spectroscopy, Kulwer Academic Publisher/Plenum Press, New York, 1999.
[4] V. Wangelin, H. Neumann, Chem. A: Eur. J. 9 (2003) 4286.
[5] J.B. Gao, Y.Y. Chen, J. Mol. Catal. A: Chem. 210 (2004) 197.
[6] M.J. Kong, A.V. Teplyakov, J. Jagmohan, J.G. Lyubovitsky, C. Mui, S.F. Bent, J. Phys. Chem. B 104 (2000) 3000.
[7] S.W. Lee, J.S. Hovis, S.K. Coulter, Surf. Sci. 462 (2000) 6.
[8] L.H. Scharpen, J.E. Wollrab, D.P. Ames, J. Chem. Phys. 49 (1968) 2368.
[9] F. Anet, D.I. Freedberg, J.W. Storer, K.N. Nouk, J. Am. Chem. Soc. 114 (1992) 10969.
[10] S.V. Shishkina, O.V. Shishkin, J. Leszczynski, Chem. Phys. Lett. 354 (2002) 428.
[11] J. Laane, J. Choo, J. Am. Chem. Soc. 116 (1994) 3889.
[12] K. Kimura, S. Katsumata, Y. Achiba, T. Yamazaki, S. Iwata, Handbook of He I Photoelectron Spectra of Fundamental Organic Molecules, Scientific Society, Tokyo, 1981.
[13] D.G. Streets, A.W. Potts, J. Chem. Soc., Faraday Trans. 70 (1974) 1505.
[14] J.K. Deng, G.Q. Li, Y. He, J.D. Huang, X.D. Wang, F. Wang, Y.A. Zhang, C.G. Ning, N.F. Gao, Y. Wang, X.J. Chen, Y. Zheng, J. Chem. Phys. 114 (2001) 882.
[15] C.G. Ning, J.K. Deng, G.L. Su, H. Zhou, X.G. Ren, Rev. Sci. Instrum. 75 (2004) 3062.
[16] K.T. Leung, C.E. Brion, Chem. Phys. 82 (1983) 87.
[17] P. Duffy, D.P. Chong, M.E. Casida, D.R. Salahub, Phys. Rev. A 50 (1994) 4707.
[18] P. Duffy, M.E. Casida, C.E. Brion, D.P. Chong, Chem. Phys. 159 (1992) 347.
[19] J.V. Ortiz, V.G. Zakizewski, O. Bolgounircheva, in: J.L. Calais, E. Kryachko (Eds.), Conceptual Perspectives in Quantum Chemistry, Kulwer Academic, New York, 1997.

[20] X.G. Ren, G.L. Su, S.F. Zhang, C.G. Ning, H. Zhou, B. Li, F. Huang, G.Q. Li, J.K. Deng, Phys. Lett. A 331 (2004) 64.
[21] M.S. Deleuze, W.N. Pang, A. Salam, R.C. Shang, J. Am. Chem. Soc. 123 (2001) 4049.
[22] C.E. Brion, Y. Zheng, J. Rokle, J.J. Neville, I.E. McCarthy, J. Wang, J. Phys. B 31 (1998) 223.
[23] X.G. Ren, C.G. Ning, J.K. Deng, S.F. Zhang, G.L. Su, F. Huang, G.Q. Li, Phys. Rev. Lett. 94 (2005) 163201.
[24] M.S. Deleuze, L.S. Cederbaum, J. Chem. Phys. 105 (1996) 7583.
[25] S. Knippenberg, K.L. Nixon, M.J. Brunger, T. Maddern, L. Campbell, N. Trout, F. Wang, W.R. Newell, M.S. Deleuze, J.P. Francois, D.A. Winkler, J. Chem. Phys. 121 (2004) 10525.